# Vibrational Energy Dependence of the Triplet Lifetime in Isolated, Photoexcited $C_{60}$

**Olof Echt,* Shaoning Yao, and Rongping Deng†**

*Department of Physics, University of New Hampshire, Durham, New Hampshire*

**Klavs Hansen**

*Department of Experimental Physics, Göteborg University and Chalmers, SE-41296 Göteborg, Sweden*

*Received: April 18, 2004; In Final Form: June 22, 2004*

We have measured the lifetime $\tau$ of the lowest triplet state $T_1$ in free $C_{60}$ by a pump−probe experiment using lasers with nanosecond pulse durations. At low pump fluence the population of $T_1$ decays with a distinct, narrow distribution of lifetimes. $\tau$ depends on the pump wavelength ($\lambda = 532$, 355, or 266 nm) as well as the temperature of the source from which $C_{60}$ is vaporized ($420 \leq T \leq 510$ °C); it ranges from 2 $\mu$s to 0.3 $\mu$s. At high pump fluence an additional lifetime as short as 40 ns is observed. A consistent correlation of all observed lifetimes with the experimental parameters is found if $\tau$ is assigned to an ensemble of $C_{60}$ ($T_1$) that has absorbed either one or two pump photons with the excess energy being randomized over all vibrational modes. Thus, $\tau = 2$ $\mu$s corresponds to a vibrational energy $E_{vib} = E_{total} - E_{triplet} = 4.6$ eV (one-photon absorption at $\lambda = 532$ nm, $T = 420$ °C) while $\tau = 40$ ns corresponds to $E_{vib} = 9.6$ eV (two-photon absorption at 355 nm, 480 °C). This result strongly suggests that delayed electrons that are emitted from highly excited $C_{60}$ ($E_{vib} \gg 10$ eV) on the time scale of ≈10 ns to 1 ms are not affected by long-lived electronically excited states. The frequently questioned description of delayed electron emission from photoexcited $C_{60}$ as thermionic emission is, therefore, warranted.

## 1. Introduction

Delayed electron emission from highly excited $C_{60}$ is readily observed unless the excitation happens on the time scale of picoseconds or shorter.[1] The phenomenon is often interpreted as thermionic emission, for example in experiments involving hyperthermal collisions of $C_{60}$ with gas-phase atoms or surfaces,[2] or excitation by lasers with pulse duration of nanoseconds or longer.[3−7]

Other authors, however, have questioned if the energy is, indeed, fully equilibrated on a time scale of ≈10 ns (for a recent summary of arguments that are critical of a thermionic emission mechanism, see ref 8). Loepfe et al.[9] used a $CO_2$ laser to desorb and excite $C_{60}$; they attributed the appearance of delayed ions to a slow transformation of excited fullerenes to geometric isomers of reduced ionization energy. Jones et al.[10] photoexcited $C_{60}$ at 193 nm after desorption with a $CO_2$ laser. They estimated that the total excitation energy was not sufficient for a purely statistical process. Zhang and Stuke observed a transition from delayed to direct ionization when the excitation laser wavelength dropped below ≈213.5 nm (5.8 eV); they concluded that delayed electron emission arises from fusion of several ($\geq 5$) long-lived triplets within a single $C_{60}$ molecule. Jackson and co-workers[11] observed delayed electron emission after electron impact excitation. They attributed the phenomenon to formation of $C_{60}$ in long-lived Rydberg states that were field-ionized. In similar experiments, however, Vostrikov and co-workers[12] did not find any evidence for field-ionization. Lutz and co-workers[13] analyzed the competition between delayed emission of $C_2$ and electrons from fullerene ions that were formed in high-energy collisions of $C_{60}$ with protons. They concluded that electrons were emitted, within $<1$ $\mu$s, from fullerene ions in long-lived electronically excited states.

The evidence quoted above is rather circumstantial and not necessarily in contradiction with a thermionic emission model,[14,15] but other recent experimental observations more stubbornly resist attempts to reconcile them with a statistical mechanism. Von Helden et al.[16] observed that an ingestion period of some 10 $\mu$s was required before delayed electron emission after IR excitation reached a maximum yield, unless the IR pulse was very intense or preceded by a weak pump pulse at 266 nm. Campbell and co-workers[17] pointed out that the temporal evolution of the delayed $C_{60}^+$ ion yield implied an unreasonably high value of the activation energy for $C_2$ loss from $C_{60}$, and that its dramatic drop after 10 $\mu$s was inconsistent with thermionic emission.

One may counter these observations with other reports according to which, under by and large similar experimental conditions, the delayed ion yield was fully consistent with a thermionic mechanism.[4,7] However, this strategy is not likely to end the debate. Instead, one should identify any mechanisms that could possibly prevent rapid energy equipartitioning between electronic and nuclear degrees of freedom, and clarify if those perceived bottlenecks persist under experimental conditions that lead to delayed ionization.

With the possible exception of Rydberg states,[11,18] there is only one candidate for an electronic state having a lifetime significantly exceeding 1 ns, namely, the lowest triplet state, $T_1$. Energy relaxation in optically excited $C_{60}$ entrained in matrixes, solutions, or $C_{60}$ films at or below room temperature has been studied by numerous authors. There is a consensus

* Author to whom correspondence should be addressed. E-mail: olof.echt@unh.edu.

† Present address: Department of Chemistry, University of Illinois at Chicago, Chicago, IL 60607-7061.

10.1021/jp048313u CCC: $27.50 
Published on Web 08/04/2004

that the initially excited singlet states nonradiatively relax into one of the lowest excited singlet states, around 2 eV, within <20 ps.[19] Further relaxation into $S_1$ and intersystem crossing into $T_1$ will occur on the time scale of ≈1 ns with a quantum yield of 1. Additional photons would be absorbed within the manifold of triplet states which, again, quickly decay nonradiatively to $T_1$.

The $S_0 \leftarrow T_1$ transition dipole moment is zero by symmetry. The transition becomes weakly allowed due to vibronic coupling, and in environments that break the $I_h$ symmetry of $C_{60}$. For temperatures below 10 K, $T_1$ lifetimes have been reported that are 410 $\mu$s in toluene,[20] 90 $\mu$s in xenon-doped neon,[21] 60 $\mu$s in krypton, and 16 $\mu$s in xenon matrixes.[22] In $C_{60}$ films, the population of singlet and triplet excitons are complex due to diffusion to defect sites, triplet−triplet annihilation, and other effects,[23] but for large delays a pure exponential decay of $T_1$ with a lifetime of 15 $\mu$s has been observed at ≈80 K.[24] As the $S_0 \leftarrow T_1$ transition becomes weakly allowed due to vibronic coupling, its rate will increase with increasing temperature, but the large environmental effects listed above make it impossible to predict the lifetime of $T_1$ in isolated $C_{60}$ from measurements in solutions or matrixes.

A first determination of the $T_1$ lifetime in isolated $C_{60}$ was reported by Smalley and co-workers[25] by resonance enhanced two photon ionization; a lifetime of 42 $\mu$s was found. Clearly, such a long lifetime would indicate a lack of coupling between electronic and nuclear degrees of freedom after photoexcitation in the UV[17] and IR.[16] Unfortunately, the excitation energy that corresponds to the lifetime observed by Smalley and co-workers was poorly defined because the $C_{60}$ beam was prepared by laser vaporization of graphite into a helium gas with subsequent supersonic expansion into vacuum. The dependence of the lifetime on the excitation energy was not explored.

Subsequently, Etheridge et al.[26] determined the temporal evolution of the absorbance of photoexcited $C_{60}$ in an argon buffer gas at 1000 K. They observed a nonexponential decay that they attributed to the distribution of vibrational energies $E_{vib}$ in $C_{60}$ at the temperature of the buffer gas; vibrational relaxation in $T_1$ was assumed to be sufficiently fast. We will argue that this assumption is inconsistent with the observation of a nonexponential decay. Thus, the functional dependence of the triplet lifetime on the vibrational energy derived from these data is questionable.

More recently, Campbell and co-workers[27] as well as our collaboration[28] essentially repeated the experiment by Smalley and co-workers[25] except that an effusive beam of $C_{60}$ was used. Both experiments were done under comparable conditions as far as the temperature of the $C_{60}$ source and the wavelength of the pump laser were concerned; both groups reported a lifetime of ≈1 $\mu$s. However, the interpretations could not have differed more. Campbell and co-workers[27] estimated the excitation energy from the observed degree of fragmentation and delayed ionization; they concluded that the lifetime remains constant over the range $15 \leq E_{vib} \leq 30$ eV. Deng et al.[28] attributed the 1 $\mu$s lifetime to a process in which only one pump photon had been absorbed; i.e., they estimated $E_{vib} = 6.5$ eV. They attributed another, much shorter lifetime at elevated pump fluence to two-photon absorption, thus concluding that $\tau$ decreases to ≈40 ns at $E_{vib} = 10$ eV.

Delayed ionization from vibrationally hot fullerenes requires the absorption of several pump photons; the vibrational excitation energy in the subensemble of $C_{60}$ that gives rise to a distinct lifetime in a pump−probe experiment is difficult to characterize in such a situation. A recent analysis suggests that, for realistic laser beam profiles, the distribution of the number of absorbed photons will be a monotonically decreasing function, even for high laser fluence.[29] Moreover, unless the pump−probe signal is measured over a large-enough dynamic range, reported lifetime(s) may be nothing but physically meaningless fit parameters. A critical test of any postulated lifetime would be to determine its dependence on *small* variations of the excitation energy. Another critical test would be to demonstrate that the results do not depend on the method by which the system is excited.

In this paper we present measurements of the pump−probe signal over a dynamic range of several orders of magnitude for $C_{60}$ source temperatures ranging from 420 to 510 °C, pump photon energies from 2.33 to 4.66 eV, and a variation of laser fluences. The observed lifetimes shorten with increasing photon energy as well as $C_{60}$ source temperature. The decrease depends approximately exponentially on the excitation energy, but not on the manner in which the energy is supplied. All observations suggest that the observed lifetimes, ranging from 2 $\mu$s to 40 ns, correspond to subensembles of $C_{60}$ that have absorbed one or, at high pump fluence, two pump photons. While the lifetimes obviously correspond to the lowest triplet state $T_1$ in these experiments, we can conclude more generally that photoexcitation of $C_{60}$ in the visible or UV does not populate any electronic states with lifetimes exceeding 40 ns once the total excess energy in the system reaches ≈11 eV. For the discussion of delayed ionization we point out that a short lifetime implies large coupling between the ground state and the triplet state. Therefore the triplet state can also be rapidly populated by thermal excitation, or excitation in the IR, from the ground state.

Our results refute the notion that delayed electron emission could possibly originate from vibrationally hot $C_{60}$ that is trapped in a long-lived electronic state.[16,17,30] Such a partly nonstatistical behavior would have important consequences for the correct assignment of values of the activation energy for $C_2$ loss from $C_{60}$.[5,31] However, in a fully equilibrated system *all* vibronic states will be populated depending on the temperature. At sufficiently high pump laser fluence this thermal population of $T_1$ (and higher states) can lead to a characteristic nonexponential decay of the pump−probe signal for which we have found some experimental evidence. Unfortunately, the contribution from one-photon excited $C_{60}$ masks this signal on the time scale that can be accessed without loss of collection efficiency, $t < 10$ $\mu$s, and we will abstain from presenting those results.

## 2. Experiment

Figure 1 shows an overview of the experimental setup. A molecular beam of $C_{60}$ is intersected at 90° by two pulsed lasers in the extraction region of a time-of-flight mass spectrometer. Ions formed as a result of laser excitation will be accelerated toward a particle detector at the end of a 0.7 m long drift tube, and recorded by a digital oscilloscope. We seek to determine the dependence of the $C_{60}^+$ ion intensity on the following experimental parameters: the time delay between pump and probe lasers, the wavelength of the pump laser, the fluence of pump and probe lasers, and the temperature $T_{C60}$ of the oven from which $C_{60}$ is vaporized.

$C_{60}$ powder (SES Research, 99.5% purity) is vaporized from a copper cell kept at a temperature ranging from 420 to 510 °C. The molecular beam is collimated to a diameter of 2 mm and irradiated by the lasers with a repetition rate of 50 Hz. The pump laser is either the second, third, or fourth harmonic of a Nd:YAG laser (wavelengths 532, 355, and 266 nm, or 2.33, 3.49, and 4.65 eV, respectively). The beam has a Gaussian

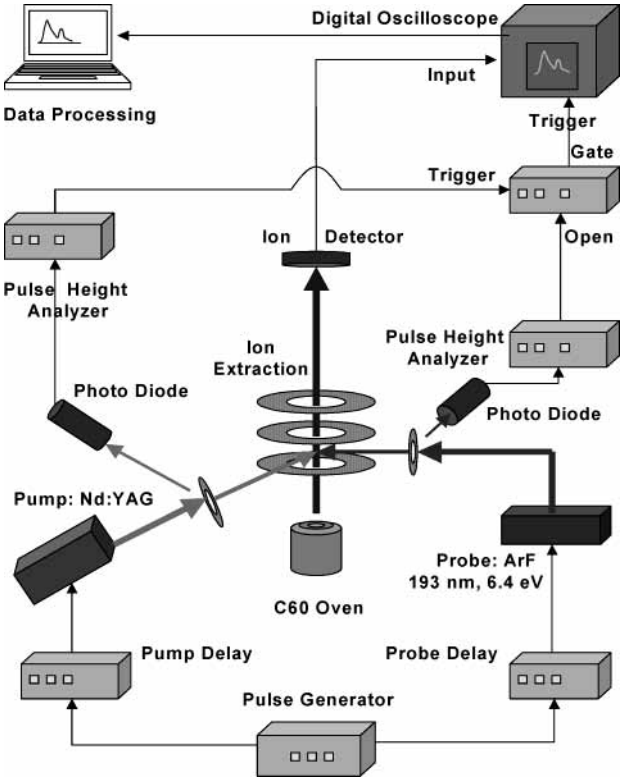


**Figure 1.** Experimental setup. The effusive $C_{60}$ beam is intersected by a Nd:YAG pump laser (operating at 532, 355, or 266 nm) and an ArF probe laser (193 nm, 6.4 eV).

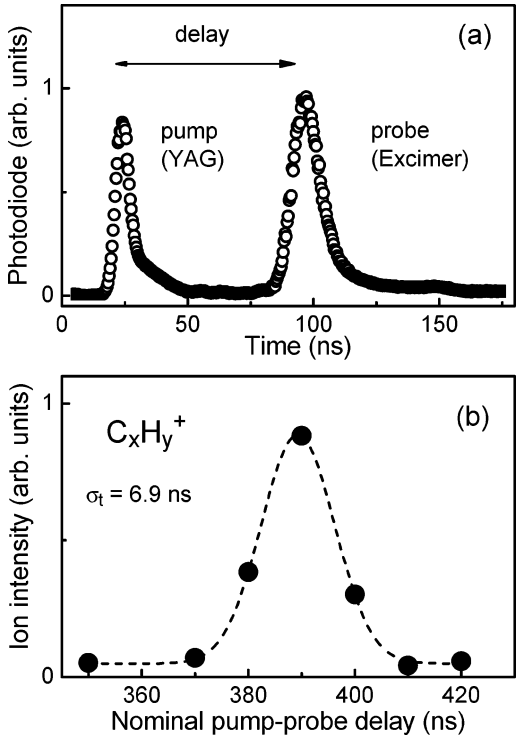


**Figure 2.** Evaluation of the experimental time resolution. (a) Pump and probe lasers monitored by a fast photodiode (spectrum averaged over 3000 laser pulses). (b) Intensity of hydrocarbon ions (mass 250 u $\leq m \leq$ 300 u) for various pump−probe delays. The Gaussian fit (dashed line) indicates a combined resolution of 6.9 ns (standard deviation).

profile. It is slightly collimated to typically 5 mm diameter and mildly focused by a planoconvex lens ($f = 52$ cm) to about 3.3 mm in the interaction region. An ArF excimer laser beam (193 nm, 6.4 eV, unfocused but collimated to a diameter of 2 mm) serves as probe.

The fluences specified below for the pump laser are estimated from the time-averaged laser intensity measured after the collimating 5 mm aperture; its spatial homogeneity in the interaction region is likely to be poor. For the very weak probe laser we measured the time-averaged laser intensity over a large ($\approx$150 mm$^2$) area and extrapolated the value to the area of the actual collimator.

A potential problem in the experiment is the loss of sensitivity, and concomitant distortion of the data, for large pump−probe delays: The ensemble of $C_{60}$ that is excited by the pump laser moves with a thermal speed of about 0.16 mm/$\mu$s, and the probe laser will miss a substantial fraction of this ensemble for large delays. From the known diameters of the laser and molecular beams, and the response of the ion signal to small ($\approx$1 mm) displacements of the probe laser beam along the molecular beam axis, we estimate that this loss of sensitivity is less than a factor of 2 for delays below 10 $\mu$s.

For very short pump−probe delays, the data will also be distorted due to the finite duration of the laser beams. In Figure 2a we show the intensity of the two lasers as seen by a fast (<1 ns rise time) photodiode. The spectrum is averaged over 3000 laser shots. The laser pulses are characterized by widths (fwhm) of 7 and 13 ns, respectively. These are only slightly broader than the single-shot laser pulses, thus demonstrating the absence of any significant jitter between the pulses.

However, the laser pulses in Figure 2a are not Gaussian. In order to determine the time resolution of the experiment more directly, we have recorded the intensity of background hydrocarbon ions in the mass range 250 u $\leq m \leq$ 300 u. These ions show a strong enhancement when the two laser pulses overlap in space and time. As shown in Figure 2b, the dependence of this enhancement (full circles) on the nominal delay between the lasers is Gaussian, with a standard deviation of 6.9 ns, or 16.2 ns fwhm. This is just slightly larger than the combined rms width of the two laser beams.

Pump−probe ion spectra for $C_{60}$ are averaged in the digital oscilloscope over a few minutes. Shot-to-shot fluctuations of the laser intensity will reduce the statistical accuracy of these spectra. Even more detrimental are slow drifts of the average laser output that occur on the time scale of minutes to hours. In the setup shown in Figure 1 we avoid these problems by monitoring the reflected laser light with fast photodiodes. Their output is sent to pulse-height analyzers (PHA) which produce a logic output only if the amplitude of the input matches a preset value within a certain range that we set to $\pm$5%. The outputs from the PHAs are combined in a logic gate which triggers the digital oscilloscope (300 MHz bandwidth, digital resolution 10 ns). With this setup, the oscilloscope is triggered only if the output of both lasers deviates less than $\pm$5% from the preset value. Fluctuations and drifts will then reduce the trigger rate, but the circuit greatly improves the reliability and statistical accuracy of the spectra.

Note that we can trigger the oscilloscope either with the light from the pump or with the probe laser. In the spectra shown here we always choose the pump laser, even for spectra that were recorded with "probe only," or with the probe fired before the pump.

### 3. Results

Figure 3 displays a set of representative ion spectra, recorded with identical sensitivity settings. The $C_{60}$ source temperature was 480 °C. The bottom spectrum was recorded with the pump

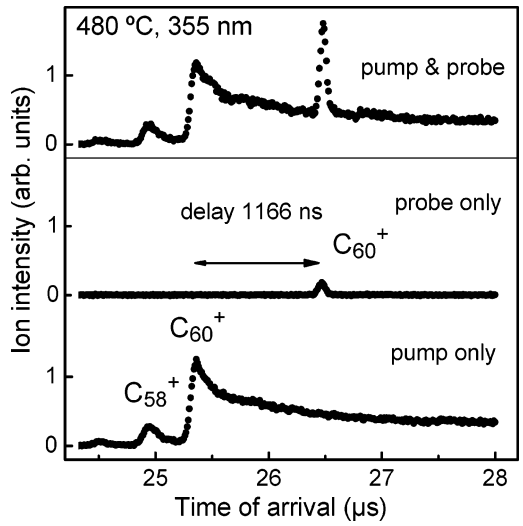


**Figure 3.** Time-of-flight spectra of fullerene ions formed by the pump laser operating at $\lambda = 355$ nm, 25 mJ/cm$^2$ (bottom panel), by the probe laser (193 nm) fired with a delay of 1166 ns (middle panel), and by pump and probe lasers (top panel). All spectra are recorded and plotted with identical sensitivities. Note the strong enhancement of the $C_{60}^+$ peak in the pump−probe spectrum over the probe-only spectrum.

laser operating at 355 nm and a fluence of about 25 mJ/cm$^2$ (2 mJ per pulse); the probe laser was blocked. The long tail following the $C_{60}^+$ ion peak is the signature of delayed ionization; it requires absorption of roughly 10 photons at this wavelength.[6] We also observe $C_{58}^+$ fragment ions at this relatively large fluence. The middle spectrum was recorded with the probe laser (193 nm, fluence 100 $\mu$J/cm$^2$, 3 $\mu$J per pulse) fired 1166 ns after the pump laser; the pump laser beam was blocked. Only a weak, prompt $C_{60}^+$ signal without any sign of delayed ionization is observed. We will later show that this probe-only signal is caused by two-photon absorption.

When both lasers are fired (Figure 3, top panel), the spectrum is the sum of the two lower spectra, except that the $C_{60}^+$ peak that arises from the probe laser is strongly enhanced. This enhancement measures the population of the lowest triplet state (or any other state that can be one-photon ionized at 193 nm) brought about by the pump laser after the chosen delay. Unless $C_{60}$ is highly excited such that those states are thermally populated to a significant extent, only long-lived electronic states can cause such an enhancement. Throughout the remainder of this work we will call this enhancement the "pump−probe signal". Note that the pump-only and probe-only spectra do not depend on the delay; they are measured only occasionally in order to verify the stability of experimental parameters (probe fluence and $C_{60}$ flux, in particular).

Figure 4 displays a series of pump−probe spectra recorded under the same conditions as in Figure 3; the pump−probe delay is varied from 7 to 1166 ns. As expected, the amplitude of the probe peak increases with decreasing delay. For very short delays ($\Delta t < 100$ ns) the probe peak rides on top of the leading edge of $C_{60}^+$ which is caused by the pump laser. We analyze this spectrum by subtracting from it the pump-only spectrum and then fitting a Gaussian.

Figure 5 (top panel) displays another series of pump−probe spectra with the pump laser operating at 532 nm (fluence 74 mJ/cm$^2$, 6.5 mJ per pulse). The absorbance of $C_{60}$ at this wavelength is low; the pump-only spectrum (bottom panel) does not show any $C_{60}^+$ ions. Therefore the $C_{60}^+$ ion peaks in the pump−probe spectra ride on top of a background that is zero, except for the small probe-only signal. The statistical accuracy

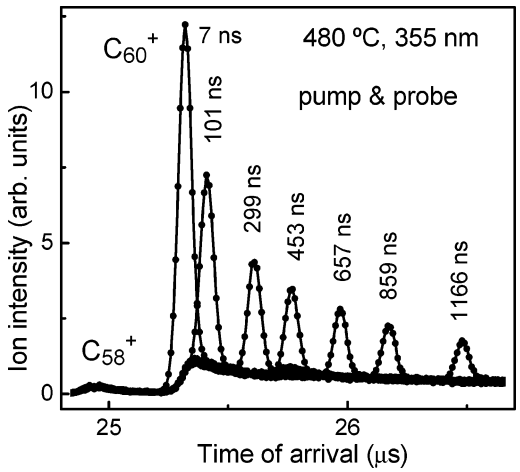


**Figure 4.** Series of pump−probe spectra superimposed on top of each other, for various pump−probe delays as indicated. The experimental conditions are identical to those in Figure 3. Lines connecting data points are drawn to guide the eye.

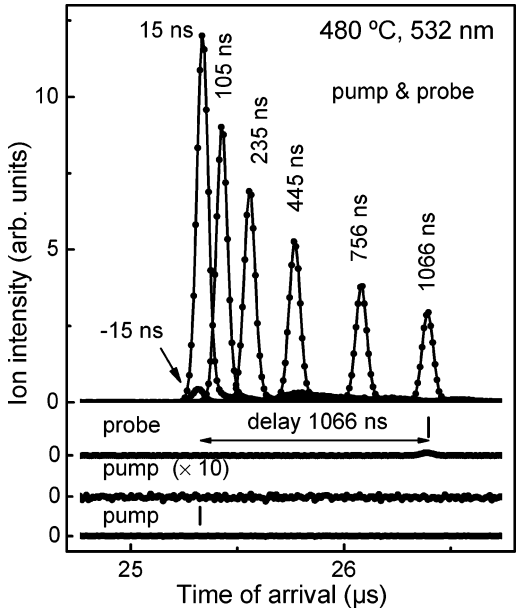


**Figure 5.** Top: Series of pump−probe spectra superimposed on top of each other, for a pump laser operating at $\lambda = 532$ nm, 74 mJ/cm$^2$. The spectra below show probe-only and pump-only spectra. Note the absence of any fullerene ions in the pump-only spectrum, even if shown with enhanced (×10) sensitivity.

of the pump−probe signal that is extracted from these data is excellent. Also note the abrupt drop of the pump−probe signal when the delay is changed from small positive (15 ns) to negative (−15 ns) values. This demonstrates the good time resolution of the setup, in agreement with the yield of hydrocarbon ions shown in Figure 2.

In Figure 6 we compile the results of analyzing several series of spectra such as those shown in Figures 4 and 5. In the top panel the pump−probe signal versus delay is plotted for three data sets, recorded with a $C_{60}$ source temperature of 480 °C but different pump wavelengths. Over a dynamic range that covers 3 orders of magnitude, the pump−probe signal decays approximately exponentially with a lifetime that decreases with increasing photon energy. In the lower panel four other data sets are plotted, recorded with a pump wavelength of 355 nm and source temperatures ranging from 420 to 510 °C. The $C_{60}$ vapor pressure increases by more than an order of magnitude over this range (see ref 6 and references therein); for clarity we

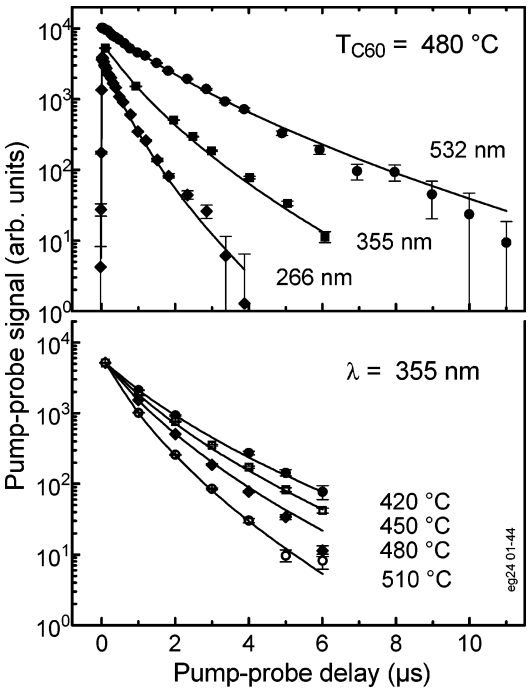


**Figure 6.** Top panel: Pump−probe signal versus pump−probe delay for spectra recorded at an identical source temperature of 480 °C but under different pump conditions (532, 355, and 266 nm at fluences of 74, 22, and 3.6 mJ/cm$^2$, respectively). Bottom panel: Pump−probe signal versus delay for identical pump conditions (355 nm, 22 mJ/cm$^2$) but different $C_{60}$ source temperatures. Solid lines result from fitting eq 1 to the data.

have scaled the intensities such that they agree for the shortest delay, $\Delta t = 0.1$ $\mu$s. Clearly, the lifetimes of the pump−probe signal decrease with increasing source temperature.

Upon closer inspection, a slight concave curvature is seen in all data sets shown in Figure 6, equivalent to a narrow distribution of lifetimes. We fit the data with

$$I(t) = \left[1 + \exp\left(-\frac{t - t_0}{1.8\sigma_t}\right)\right]^{-1} A \int \exp\left[-\frac{1}{2}\left(\frac{\ln \tau - \ln \tau_0}{\sigma_{\ln \tau}}\right)^2\right] \times \exp\left(-\frac{t}{\tau}\right) \mathrm{d}(\ln \tau) \quad (1)$$

The first factor on the right-hand side of eq 1 is a step function that switches at $t_0$ from zero to one with an abruptness determined by $\sigma_t$. More specifically, $\sigma_t$ is the standard deviation of the derivative of the step function. The integral describes an exponential decay with a distribution of lifetimes that is Gaussian on a logarithmic scale, centered at ln $\tau_0$ with a width $\sigma_{\ln \tau}$.

As indicated by the solid lines in Figure 6 (top), all data sets are described well by eq 1 with mean lifetimes $\tau_0$ that decrease from 1.2 $\mu$s at 532 nm to 0.35 $\mu$s at 266 nm. The fit parameter $\sigma_{\ln \tau}$ exhibits considerable scatter. After a preliminary fitting of several data sets we have chosen a common value of $\sigma_{\ln \tau} = 0.47$ for all final fits. In other words, 68% of the values in the distribution of lifetimes differ from $\tau_0$ by less than a factor of $\exp(\sigma_{\ln \tau}) = 1.6$. The physical origin of this distribution will be discussed later.

For clarity, only one data set in Figure 6 (266 nm, 480 °C) is shown with negative pump−probe delays, together with the complete fit expression (eq 1). From this and several other sets we derive $\sigma_t \approx 7$ ns, which agrees nicely with the resolution obtained from the intensity of hydrocarbon ions shown in Figure 2.

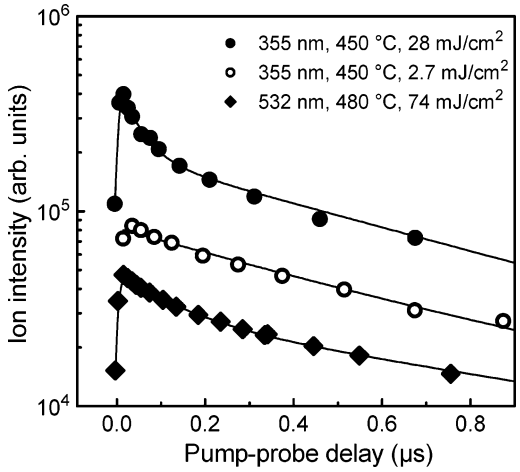


**Figure 7.** Circles: Pump−probe signal versus delay for a pump wavelength of 355 nm recorded with low and high fluence (open and filled circles, respectively). Diamonds: Pump wavelength 532 nm, 74 mJ/cm$^2$. Two distinct exponentials are required to fit the high-fluence data (filled symbols).

The pump fluence does not affect the time dependence of the pump−probe signal unless the fluence becomes large. In Figure 7 we show two data sets recorded with a pump wavelength of 355 nm, for fluences of 2.7 and 28 mJ/cm$^2$ (open and filled circles, respectively). At low fluence a single lifetime of 0.74 $\mu$s is observed (the curvature of the fitted line is hardly discernible here because only a narrow time range is displayed). At high fluence an additional lifetime, $\tau = 0.044$ $\mu$s, appears; the longer lifetime remains unchanged. Similarly, at 532 nm and 74 mJ/cm$^2$ a lifetime $\tau_0 \approx 0.23$ $\mu$s becomes apparent, in addition to the lifetime $\tau_0 = 1.2$ $\mu$s that was observed at low fluence (Figure 6). Note that the ratios of the two lifetimes, either 0.74/0.044 or 1.2/0.23, are considerably larger than the exponential of the width, $\exp(\sigma_{\ln \tau}) = 1.6$, that characterizes the low-fluence data. Hence, it is proper to discuss the high-fluence data in terms of bimodal distributions of lifetimes.

In view of these results one might also expect a very short lifetime for high pump fluence at 266 nm. We have not seen any evidence for it. Perhaps the maximum possible laser fluence, 4 mJ/cm$^2$, was insufficient. Alternatively, an additional lifetime at 266 nm will be comparable to or less than the experimental time resolution, rendering it unobservable.

In Figure 8 we compile all lifetimes deduced from the data shown in Figures 6 and 7, and from other data sets. The $C_{60}$ source temperature is indicated on the abscissa. Lines connect data points that were recorded with identical pump wavelength. Open symbols refer to measurements at low to modest pump fluence; filled symbols denote lifetimes seen at high pump fluence. Except for the value $\tau_0 = 0.044$ $\mu$s the uncertainties of $\tau_0$ reported by the fits are smaller than the size of the symbols. We estimate an uncertainty of ≈10% for the lifetimes determined at low fluence. The uncertainty is caused by a significant correlation between the $\sigma_{\ln \tau}$ value used in the fit and the resulting value of $\tau_0$. An uncertainty of 10% is also consistent with the scatter between pairs of values from repeated measurements shown for $\lambda = 355$ nm at 420 and 450 °C. The uncertainties of the additional, shorter lifetimes observed at high fluence may be larger. The statistical error of the source temperature is small, but a systematic error of a few degrees cannot be excluded.

For the following discussion it will be useful to distinguish between one-photon and multiphoton processes. In Figure 9 (top) we show a double logarithmic plot of the probe fluence

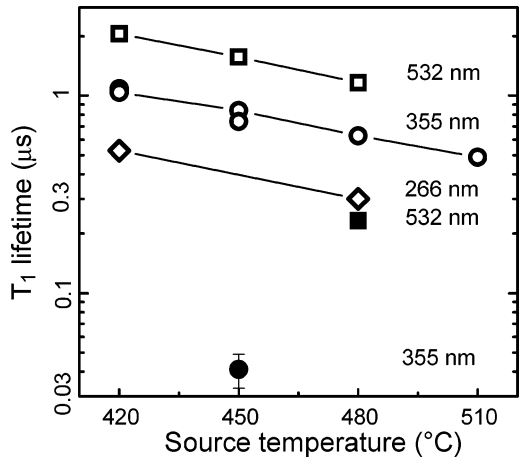


**Figure 8.** Summary of lifetimes deduced from pump−probe data versus $C_{60}$ source temperature, for pump wavelengths as indicated. Open symbols indicate lifetimes recorded with low pump fluence. Filled symbols indicate additional lifetimes observed at high pump fluence; they arise from two-photon absorption.

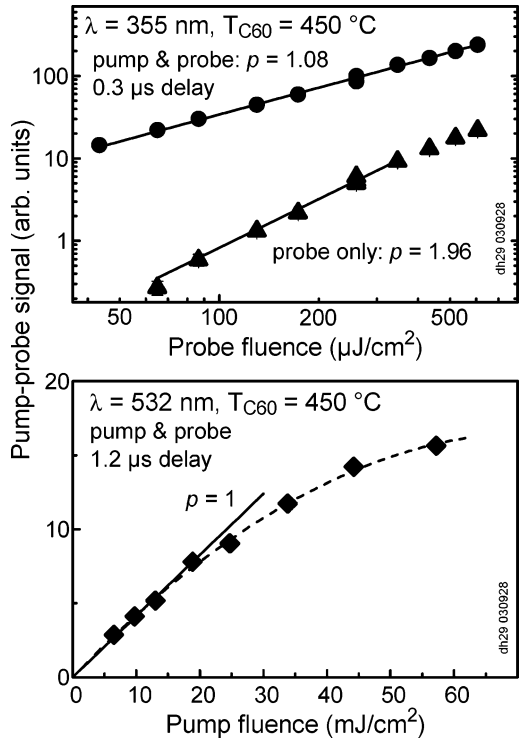


**Figure 9.** Upper panel: Pump−probe signal (circles) and probe-only signal (diamonds) versus probe fluence. The slope of the fitted power law (solid lines) is approximately 1 and 2, respectively. Lower panel: Pump−probe signal versus pump fluence for a pump−probe delay of 1.2 $\mu$s. The dependence at low pump fluence is approximately linear.

dependence of the pump−probe signal evaluated at a delay of 0.3 $\mu$s. Fitting a power law (solid line) we find a slope of 1.08 $\pm$ 0.02, indicating that a single probe photon ionizes $C_{60}$ out of the triplet state, as expected. We have obtained similar fluence dependences for longer pump−probe delays. The slope for the probe-only ion intensity is 1.96 $\pm$ 0.03, in agreement with the expectation that one photon will pump $C_{60}$ into the triplet state, and another will ionize.

In the bottom panel of Figure 9 we show the dependence of the pump−probe signal on the pump fluence evaluated for a delay of 1.2 $\mu$s and $\lambda_{pump} = 532$ nm. The dashed curve is drawn to guide the eye. As shown by the solid line, the slope of the data is consistent with a value of 1.0 for low fluence.

## 4. Discussion

We begin with a summary of the experimental results:

1. For low to modest pump fluence, the pump−probe signal versus pump−probe delay is described well by a narrow distribution of lifetimes.

2. The mean lifetime of these distributions, $\tau_0$, decreases with increasing pump photon energy and increasing $C_{60}$ source temperature. Observed values range from 2.0 to 0.3 $\mu$s.

3. $\tau_0$ does not depend on the pump fluence. However, at high fluences an additional, much shorter lifetime (or narrow distribution of lifetimes) is observed.

4. The time resolution of our setup precludes the observation of lifetimes below $\approx$0.01 $\mu$s. However, we would be able to identify any significant population of long-lived states ($\tau \gg 2$ $\mu$s) by the pump laser. The only condition under which such a long-lived pump−probe signal appears is for maximum laser fluence (see Figure 2 in ref 28). This effect is likely due to highly excited $C_{60}$ in which the triplet state is thermally populated.

These results suggest that the lowest triplet state is efficiently populated by photon absorption, and that its lifetime decreases with increasing vibrational energy content that we express as follows:

$$E_{\mathrm{vib,T1}} = E(T_{C60}) + nh\nu - E_{\mathrm{T1}} \qquad (2)$$

where $E(T_{C60})$ is the average internal (vibrational) energy of $C_{60}$ as it emerges from the source at temperature $T_{C60}$, $n$ denotes the number of absorbed pump photons, $h\nu$ their energy, and $E_{T1}$ the energy of the triplet state. We have computed $E(T_{C60})$ from the set of vibrational frequencies published by Schettino et al.[32] From a quadratic fit to these data from 600 to 1200 K we obtain the relation

$$E(T_{C60})/\mathrm{eV} = -2.550 + 0.00737T/K + 2.6523 \times 10^{-6}(T/K)^2 \qquad (3)$$

which differs from the exact energies by less than 0.02 eV. For $E_{T1}$ we adopt a value of 1.57 eV.[33]

How many pump photons are absorbed? The answer can be obtained from the low-fluence data (open symbols) in Figure 8. There are two data points with lifetimes of $\tau \approx 0.5$ $\mu$s, one obtained at 420 °C and 266 nm, the other at 510 °C, 355 nm. The difference in thermal energy (eq 3) between these two temperatures is 1.02 eV, which closely matches the difference in the one-photon energies, 4.66−3.49 = 1.17 eV. Hence, a unique relation between vibrational energy $E_{\mathrm{vib,T1}}$ and the observed lifetime $\tau$ requires that we assign $n = 1$ to all low-fluence data. In other words, the triplet state is populated by absorption of exactly one pump photon. This conclusion agrees with the observation that the pump−probe signal depends on the first power of the pump fluence (Figure 9, bottom panel).

It is tempting to assume that the additional, shorter lifetimes observed at high fluence (filled symbols in Figure 8) are due to absorption of two photons. This hypothesis can be tested: For identical temperatures a low-fluence lifetime observed at 266 nm should agree with the additional lifetime observed at 532 nm, high-fluence. The lifetimes determined at 480 °C indeed pass this test.

With this interpretation we can plot all lifetimes versus vibrational excess energy; the result is shown in Figure 10. On this semilogarithmic plot the data fall on a common straight line for energies spanning a range of 4.6 to 9.6 eV, or lifetimes

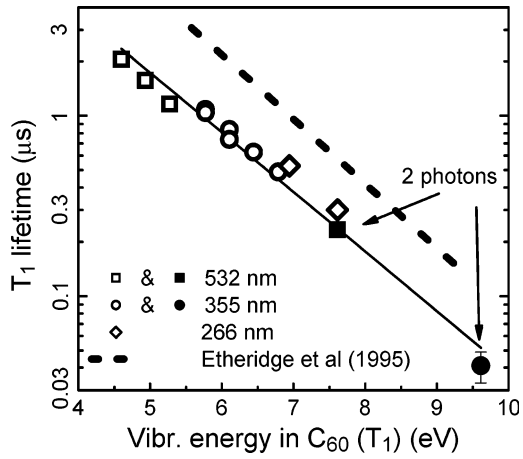


**Figure 10.** Compilation of all triplet lifetimes shown in Figure 8, versus vibrational energy in $C_{60}$ ($T_1$) computed with the help of eq 3, together with a fit (solid line) that assumes an exponential energy dependence. The dashed line indicates lifetimes reported by Etheridge et al.[26]

covering nearly 2 orders of magnitude. From a fit to these data we obtain

$$\tau = \beta \exp(-\alpha E_{\mathrm{vib,T1}}) \tag{4}$$

with

$$\beta = 78.3 \pm 9.7\ \mu\mathrm{s}$$

and

$$\alpha = 0.76 \pm 0.02\ \mathrm{eV}^{-1}$$

This relation can be checked against an earlier result, the distribution of lifetimes expressed as $\sigma_{\ln \tau}$. The obvious source of this distribution is the distribution of vibrational energies in the effusive beam of $C_{60}$. For the temperatures considered here, the energy distribution will be Gaussian of width $\sigma_E$, and we can write the triplet population as

$$P(t) = A\int \exp\left[-\frac{1}{2}\left(\frac{E - E_{\mathrm{vib,T1}}}{\sigma_E}\right)^2\right]\exp\left(-\frac{t}{\tau(E)}\right) \mathrm{d}E = A\int \exp\left[-\frac{1}{2}\left(\frac{\ln \tau(E) - \ln \tau_0}{\alpha\sigma_E}\right)^2\right]\exp\left(-\frac{t}{\tau(E)}\right) \mathrm{d}E \tag{5}$$

where eq 4 was used in the last step. The logarithm of lifetimes is normal distributed on an energy scale with a most probable value $\tau_0 = \tau(E_{\mathrm{vib,T1}})$ and a width $\alpha\sigma_E$.

Furthermore, from eq 4 one has $\mathrm{d}E = \mathrm{const}\ \mathrm{d}(\ln \tau)$, which renders eq 5 equal to eq 1 (without the step function), provided that $\alpha\sigma_E = \sigma_{\ln \tau}$. Do our experimental results confirm this? For constant heat capacity one has $\sigma_E = T(k_B C)^{1/2}$, where $C(T)$ is the vibrational heat capacity that one may compute from eq 3.[34] Thus, $\alpha\sigma_E$ should increase from 0.51 at 420 °C to 0.59 at 510 °C. A calculation of the same quantities based on the level density gives only slightly higher values, 0.54 and 0.62, respectively. These values agree quite nicely with the value $\sigma_{\ln \tau} = 0.47$ that we had obtained by fitting eq 1 to the data shown in Figure 6. The expected variation of $\sigma_{\ln \tau}$ with $T$ is, however, too small to be identified in the data.

In Figure 10 we also show the lifetime $\tau(E_{\mathrm{vib,T1}})$ that Etheridge et al.[26] deduced from the time-dependent absorbance $A(t)$ of gas-phase $C_{60}$ after excitation at 532 nm. Their lifetimes are larger than ours by a factor of two to three, or, viewed differently, they are shifted to higher energies by more than 1 eV. Those experiments were performed at 706 to 767 °C in an argon buffer gas. $\tau(E)$ was not, as in our experiment, derived from the dependence of the mean lifetime on temperature, but from the functional dependence of $A(t)$ which revealed a wide distribution of lifetimes that, from our considerations above, would be $\sigma_{\ln \tau} = 0.79$ at 1000 K.

An important factor in the experiments by Etheridge et al. is the presence of a buffer gas which collisionally cools the $C_{60}$. The authors mention that they did not observe any change in the evolution of the absorbance when they reduced the argon pressure from 100 to 1 Torr. They conclude that the excess vibrational energy generated during $T_1 \leftarrow S_n$ radiationless decay, $h\nu - E_{T1} = 0.76$ eV, is "collisionally relaxed within the triplet lifetime".[26] The shortest lifetime reported by the authors was 0.15 $\mu$s, hence their conclusion implies a vibrational relaxation rate greatly exceeding $7 \times 10^6\ \mathrm{s}^{-1}$. It is true that collisional vibrational relaxation of aromatic molecules in $T_1$ can be an order of magnitude more efficient than in $S_0$.[35] However, it is difficult to grasp how a relaxation rate much larger than $7 \times 10^6\ \mathrm{s}^{-1}$ can be achieved when the rate of Ar−$C_{60}$ collisions is only $5 \times 10^6\ \mathrm{s}^{-1}$ at 1 Torr and 1000 K.

In fact, the assumption of rapid collisional cooling should be questioned in a more fundamental way: it directly contradicts the nonexponential decay of $A(t)$. Rapid collisional relaxation implies that the ensemble of $C_{60}(T_1)$ is canonical as far as the vibrational energy is concerned. Hence, for the subensemble in the $T_1$ state, the quantity $A(t)^{-1}\ \mathrm{d}A(t)/\mathrm{d}t$ is independent of time, which implies a single exponential for $A(t)$. The deviation from a single exponential that we observe in our experiments under collisionless conditions (Figures 6 and 7) arises from the fact that the high-energy tail of the vibrational energy distribution depletes faster than the low-energy tail. This depletion cannot possibly occur in an environment that is claimed to ensure rapid energy exchange.

Several factors may have conspired in the experiments by Etheridge et al.[26] to cause a curvature in $A(t)$. If collisional cooling were much slower than assumed, then the procedure used in the data analysis would have been correct, but the vibrational energies assigned to $\tau(E)$ should be increased by 0.76 eV, thus increasing the discrepancy between their data and ours in Figure 10 to ≈2 eV. Additionally, their assumption of a distinct temperature is questionable. The authors mention that the "temperature profile along the cell axis gave an effective optical path length of approximately 5 cm, beyond which the $C_{60}$ vapor condensed onto the quartz tube...." The effect of this temperature gradient on the distribution of lifetimes was ignored in the data analysis.

What are the implications of our results for the mechanism of delayed electron emission from $C_{60}$? As mentioned in the Introduction, it has been suggested that delayed electrons could originate from $C_{60}$ trapped in a long-lived electronic state. $T_1$ would be the prime candidate because, barring Rydberg states, it is the only long-lived state at low temperature, and it is populated with 100% efficiency after photoexcitation in the visible or UV. This scenario would render a statistical description invalid.[8]

In general, other mechanisms for delayed electron emission are conceivable[8] but, for $C_{60}$, the process clearly requires high excitation energies. For example, a pump-only study[6] at 355 nm shows that the yield of delayed electrons initially increases with the 6th power of the laser fluence equivalent to the absorption of ≥21 eV. Unless one postulates intramolecular fusion of ≥5 excitons,[14,30] one has to accept that delayed electron emission is thermally activated. Electron emission from $T_1$

would then be much more efficient than from a statistical ensemble because of the reduction in the activation energy from 7.6 to ≈6.0 eV.

In the present work we have demonstrated that the $T_1$ lifetime decreases monotonically to ≈40 ns at $E_{vib,T1} = 9.6$ eV (total energy 11.2 eV). Even if the lifetime of $T_1$ would not decrease any further with increasing excitation energy, the system would be fully statistical on the time scale of most experiments and electron emission could be described as true thermionic emission. Only one scenario would invalidate this conclusion, namely, an eventual increase of $\tau_{T1}$ with increasing excitation energy. This appears to be extremely unlikely. Although the $T_1$ lifetime in aromatic molecules may, after an initial steep decline with increasing excitation energy, approach some constant value (see ref 36 and references therein), we are not aware of any system that exhibits an increase of $\tau_{T1}$ with increasing energy, nor can we think of a physical reason for such a reversal.

We now turn to the report by Meijer and co-workers[16] concerning electron emission from IR heated $C_{60}$. The authors used a 4 $\mu$s wide pulse from a free electron laser to resonantly excite $C_{60}$ via vibrations at ≈520 $cm^{-1}$. For low laser fluence the electron yield increased slowly until it reached a maximum some 50 $\mu$s after the IR pulse. It was concluded that reaching the $T_1$ state is a high hurdle on the way from hot molecules to ions. Only at high fluence, or when pre-exciting the fullerenes with a weak UV pulse (266 nm) 5 $\mu$s before the IR pulse, the spectrum would exhibit the usual behavior of an abrupt rise followed by a monotonic decay. We cannot explain these features, but two remarks are warranted. First, in a conceptually similar experiment involving excitation near 1000 $cm^{-1}$, Quack and co-workers[4] did not observe such a slow onset of the delayed electron signal. By varying the laser pulse duration while keeping the fluence constant they demonstrated the absence of an intrinsic nonlinear intensity dependence and, thus, the dominance of vibrational preionization. A possible way to reconcile the differences between the observations by Hippler et al.[4] and von Helden et al.[37] would be to assume that the modes excited at 520 $cm^{-1}$ do not quickly relax into other vibrational modes, but this contradicts the notion that "it is safe to assume that the IVR process is much faster than the rate of photon absorption."[37] Second, in a subsequent, more detailed experiment Meijer and co-workers concluded[38] that, after preexcitation at 266 nm with laser pulses of 30 ps duration, the system quickly returns to the electronic ground state before it is probed with the IR laser pulse a few microseconds later. Indeed, as seen from Figure 8, the $T_1$ lifetime after absorption of a 266 nm photon is less than 0.5 $\mu$s for typical temperatures.

The data presented here do not give any information on the reason for the exponential decrease in lifetime with excitation energy, nor of the mechanism through which $T_1$ decays. Several authors have addressed the question, mainly in connection with similar problems in smaller organic molecules (see e.g. refs 36, 39, and 40). The trend for these small molecules is a lifetime decreasing with increasing excitation energy, similar to the one observed here. Morse et al.[36] suggest a finite lifetime due to a direct decay from the triplet to the singlet state. The transition rates will then be partly determined by the Franck−Condon factor as a multiplicative factor. The excitation energy dependence of the rate constant appears as the result of the combined effect of these factors. An application of this method to our data would be less than straightforward. One problem is the fact that $C_{60}$ is prepared in a state with a thermal energy which is relatively large compared with the energy released when the triplet state decays. Although some theoretical calculations of the vibrational modes of the triplet state have appeared,[41] these difficulties have prevented us from exploring the suggestion of Morse et al.[36] further.

Alternatively, the decay of $T_1$ in pyrazine has been ascribed to an activated process which involves excitation from $T_1$ to higher triplet states.[40] This seems to reproduce the pyrazine data quite well, but requires the introduction of a finite zero-temperature contribution to the decay rate constant. It is possible to rationalize the present data on $C_{60}$ to some extent with a model of similar nature. If the decay of $T_1$ occurs via the thermally populated $S_1$ with a rate constant $S_0 \leftarrow S_1$ which is independent of excitation energy, the lifetime is determined, up to a constant, by the ratio of the populations of $S_1$ and $T_1$ alone. This gives an energy dependence of $\rho(E - E_{S1})/\rho(E - E_{T1})$, where $\rho$ is the vibrational level density, $E$ the total excitation energy, and $E_{S1}$ and $E_{T1}$ are the energies of $S_1$ and $T_1$, respectively. In terms of the microcanonical temperature $T = T(E - E_{T1})$, the relation becomes $k \propto \exp[(E_{S1} - E_{T1})/T]$. The virtue of this suggestion is that it provides a natural explanation of the magnitude of the characteristic energy scale observed in the data, 1.3 $eV^{-1}$ (see eq 4), in terms of the heat capacity of the molecule, the temperature, and the $S_1 - T_1$ energy difference. The model predicts a value of $d \ln(k)/dE$ equal to $d \ln(\rho(E - E_{S1})/\rho(E - E_{T1}))/dE$. Calculations of the vibrational level density give the values 0.71 $eV^{-1}$ for the interval 5−7 and 0.36 $eV^{-1}$ for the interval 8−10 eV, compared with the experimental value of 0.76 $eV^{-1}$. The drawback is that the model cannot account for the low-temperature lifetimes seen in cryogenic experiments[20−22] without invoking an additional direct rate constant similar to the one of Terazima et al.[40] Also, the decay from $S_1$ to $S_0$ is as yet unspecified. In spite of these shortcomings, the similarity of the model energy scale with the experimental scale is close enough to be pursued further. The idea can be tested with a measurement of the decay of the triplet state in $C_{70}$. If the mechanism is similar for that molecule, the model prediction is that the lifetime decreases roughly exponentially with excitation energy, with an energy scale which is similar to the one for $C_{60}$.

## 5. Conclusion

We have shown, with pump−probe experiments, that the $T_1$ state of $C_{60}$ decays exponentially with a time constant which depends on the vibrational excitation energy of the molecule. The energy dependence is also exponential, with a characteristic energy of 0.76 $eV^{-1}$. The internal energy of the molecule was changed by varying both the source temperature and the photon energy of the pump laser. The measured lifetimes were found to be independent of the method by which the excess vibrational energy was introduced into the molecule, proving that the equilibration of all other degrees of freedom proceeds faster than the decay of the triplet state. This also allowed the unambiguous assignment of the number of absorbed photons associated with a specific lifetime.

**Acknowledgment.** O.E. thanks E. E. B. Campbell and co-workers for the hospitality during his stay at Chalmers, where this manuscript was prepared. This work was supported by the National Science Foundation under Grant No. 9507959 and the Air Force Office of Scientific Research under Grant No. F49620-98-1-0499.

## References and Notes

(1) Zhang, Y.; Späth, M.; Krätschmer, W.; Stuke, M. *Z. Phys. D* **1992**, *23*, 195. Campbell, E. E. B.; Hoffmann, K.; Hertel, I. V. *Eur. Phys. J. D* **2001**, *16*, 345.

(2) Wan, Z.; Christian, J. F.; Basir, Y.; Anderson, S. L. *J. Chem. Phys.* **1993**, *99*, 5858. Yeretzian, C.; Beck, R. D.; Whetten, R. L. *Int. J. Mass Spectrom. Ion Processes* **1994**, *135*, 79. Weis, P.; Rockenberger, J.; Beck, R. D.; Kappes, M. M. *J. Chem. Phys.* **1996**, *104*, 3629. Fiegele, T.; Echt, O.; Biasioli, F.; Mair, C.; Märk, T. D. *Chem. Phys. Lett.* **2000**, *316*, 387. Campbell, E. E. B.; Rohmund, F. *Rep. Prog. Phys.* **2000**, *63*, 1061. Deng, R.; Echt, O. *Int. J. Mass Spectrom.* **2004**, *233*, 1.

(3) Wurz, P.; Lykke, K. R. *J. Phys. Chem.* **1992**, *96*, 10129. Campbell, E. E. B.; Tittes, A.; Drantz, D.; Schneider, R.; Hielscher, A. *Chem. Phys. Lett.* **1991**, *184*, 404. Campbell, E. E. B.; Ulmer, G.; Hertel, I. V. *Z. Phys. D* **1992**, *24*, 81. Ding, D.; Compton, R. N.; Haufler, R. E.; Klots, C. E. *J. Phys. Chem.* **1993**, *97*, 2500. Ding, D.; Huang, J.; Compton, R. N.; Klots, C. E.; Haufler, R. E. *Phys. Rev. Lett.* **1994**, *73*, 1084. Lepine, F.; Climen, B.; Pagliarulo, F.; Baguenard, B.; Lebeault, M. A.; Bordas, C.; Heden, M. *Eur. Phys. J. D* **2003**, *24*, 393.

(4) Hippler, M.; Quack, M.; Schwarz, R.; Seyfang, G.; Matt, S.; Märk, T. D. *Chem. Phys. Lett.* **1997**, *278*, 111.

(5) Hansen, K.; Echt, O. *Phys. Rev. Lett.* **1997**, *78*, 2337.

(6) Deng, R.; Echt, O. *J. Phys. Chem. A* **1998**, *102*, 2533.

(7) Tomita, S.; Andersen, J. U.; Hansen, K.; Hvelplund, P. *Chem. Phys. Lett.* **2003**, *382*, 120.

(8) Campbell, E. E. B.; Levine, R. D. *Annu. Rev. Phys. Chem.* **2000**, *51*, 65.

(9) Loepfe, M.; Siegmann, H. C.; Sattler, K. *Z. Phys. D* **1993**, *26*, S311.

(10) Jones, A. C.; Dale, M. J.; Banks, M. R.; Gosney, I.; Langridge-Smith, P. R. R. *Mol. Phys.* **1993**, *80*, 583.

(11) Gallogly, E. B.; Bao, Y. H.; Han, K. L.; Lin, H.; Jackson, W. M. *J. Phys. Chem.* **1994**, *98*, 3121.

(12) Vostrikov, A. A.; Dubov, D. Y.; Agarkov, A. A. *Tech. Phys. Lett.* **1995**, *21*, 715.

(13) Reinkoster, A.; Werner, U.; Kabachnik, N. M.; Lutz, H. O. *Phys. Rev. A* **2001**, *64*, 023201.

(14) Lykke, K. R. *Phys. Rev. Lett.* **1995**, *75*, 1234.

(15) Klots, C. E.; Compton, R. N. *Phys. Rev. Lett.* **1996**, *76*, 4092. Klots, C. E.; Compton, R. N. *Surf. Rev. Lett.* **1996**, *3*, 535.

(16) von Helden, G.; Holleman, I.; van Roij, A. J. A.; Knippels, G. M. H.; van der Meer, A. F. G.; Meijer, G. *Phys. Rev. Lett.* **1998**, *81*, 1825.

(17) Rohmund, F.; Heden, M.; Bulgakov, A. V.; Campbell, E. E. B. *J. Chem. Phys.* **2001**, *115*, 3068.

(18) Wesdorp, C.; Robicheaux, F.; Noordam, L. D. *Chem. Phys. Lett.* **2000**, *323*, 192. Boyle, M.; Hoffmann, K.; Schulz, C. P.; Hertel, I. V.; Levine, R. D.; Campbell, E. E. B. *Phys. Rev. Lett.* **2001**, *87*, 273401.

(19) Stepanov, A. G.; Portella-Oberli, M. T.; Sassara, A.; Chergui, M. *Chem. Phys. Lett.* **2002**, *358*, 516.

(20) Wasielewski, M. R.; O'Neil, M. P.; Lykke, K. R.; Pellin, M. J.; Gruen, D. M. *J. Am. Chem. Soc.* **1991**, *113*, 2774.

(21) Hung, W.-C.; Ho, C.-D.; Liu, C.-P.; Lee, Y.-P. *J. Phys. Chem.* **1996**, *100*, 3927.

(22) Sassara, A.; Zerza, G.; Chergui, M. *Chem. Phys. Lett.* **1996**, *261*, 213.

(23) Yang, S. I.; Suh, Y. D.; Jin, S. M.; Kim, S. K.; Park, J.; Shin, E. J.; Kim, D. *J. Phys. Chem.* **1996**, *100*, 9223. Jacquemin, R.; Kraus, S.; Eberhardt, W. *Solid State Commun.* **1998**, *105*, 449.

(24) Long, J. P.; Chase, S. J.; Kabler, M. N. *Chem. Phys. Lett.* **2001**, *347*, 29.

(25) Haufler, R. E.; Wang, L. S.; Chibante, L. P. F.; Jin, C.; Conceicao, J.; Chai, Y.; Smalley, R. E. *Chem. Phys. Lett.* **1991**, *179*, 449.

(26) Etheridge, H. T.; Averitt, R. D.; Halas, N. J.; Weisman, R. B. *J. Phys. Chem.* **1995**, *99*, 11306.

(27) Heden, M.; Bulgakov, A. V.; Mehlig, K.; Campbell, E. E. B. *J. Chem. Phys.* **2003**, *118*, 7161.

(28) Deng, R.; Treat, M.; Echt, O.; Hansen, K. *J. Chem. Phys.* **2003**, *118*, 8563.

(29) Mehlig, K.; Hansen, K.; Heden, M.; Lassesson, A.; Bulgakov, A. V.; Campbell, E. E. B. *J. Chem. Phys.* **2004**, *120*, 4281.

(30) Zhang, Y.; Stuke, M. *Phys. Rev. Lett.* **1993**, *70*, 3231. Stuke, M.; Zhang, Y. *Phys. Rev. Lett.* **1995**, *75*, 1235.

(31) Lifshitz, C. *Int. J. Mass Spectrom.* **2000**, *198*, 1.

(32) Schettino, V.; Pagliai, M.; Ciabini, L.; Cardini, G. *J. Phys. Chem. A* **2001**, *105*, 11192.

(33) Guldi, D. M.; Kamat, P. In *Fullerenes: Chemistry, Physics, and Technology*; Kadish, K. M., Ruoff, R. S., Eds.; John Wiley & Sons: New York, 2000; p 225.

(34) Schroeder, D. V. *Introduction to Thermal Physics*; Addison-Wesley: San Francisco, 2000.

(35) Wu, F.; Weisman, R. B. *J. Chem. Phys.* **1999**, *110*, 5047.

(36) Morse, M. D.; Puiu, A. C.; Smalley, R. E. *J. Chem. Phys.* **1983**, *78*, 3435.

(37) von Helden, G.; Holleman, I.; Meijer, G.; Sartakov, B. *Opt. Express* **1999**, *4*, 46.

(38) van Heijnsbergen, D.; von Helden, G.; Sartakov, B.; Meijer, G. *Chem. Phys. Lett.* **2000**, *321*, 508.

(39) Freed, K. F. *Acc. Chem. Res.* **1978**, *11*, 74.

(40) Terazima, M.; Yamauchi, S.; Hirota, N. *J. Phys. Chem.* **1986**, *90*, 4294.

(41) Hara, T.; Nomura, Y.; Narita, S.; Ito, H.; Shibuya, T. *J. Mol. Struct. (THEOCHEM)* **2002**, *589*, 139.